論文

Collision Avoidance Maneuver Simulation of Tilt Rotor Unmanned Aerial Vehicle

Soojung Hwang*, Myeong Kyu Lee** and Soohun Oh***

틸트로터 무인기의 충돌회피기동 모사

황수정*, 이명규**, 오수훈***

ABSTRACT

The collision avoidance maneuver flight simulation for tilt rotor unmanned aerial vehicle was performed by time-accurate numerical integration method based on wind tunnel test data. Five representative collision avoidance maneuvers were simulated under constraints of aerodynamic stall, propulsion power, structural load, and control actuator capability. The collision avoidance performances of the maneuvers were compared by the computed collision avoidance times. The sensitivities of initial flight speed and collision zone shape on the collision avoidance time were investigated. From these results, it was found that the moderate pull-up turn maneuver defined using moderate pitch and maximum roll controls within simulation constraints is the most robust and efficient collision avoidance maneuver under the various flight speeds and collision object shapes in the tilt rotor UAV applications.

Key Words : Collision Avoidance Maneuver, Tilt Rotor, Unmanned Aerial Vehicle

Ⅰ. Introduction

Many researches of collision avoidance methodology for automated airspace concept have been made to ensure the safety and efficiency in air traffics (Ref. 1 and 2). Currently Air Traffic Control (ATC) is a completely centralized system where individual aircraft have little freedom to choose more optimal route, altitude and speed. Aircrafts are traveling along predefined jet-ways or corridors. Although this approach has worked satisfactory in the past and resulted relatively safe, the enormous increase in the demands for air transportation would required more efficient utilization of airspace (Ref. 3). One of proposals to increase the efficiency is the innovative concept of free flight (Ref. 4).

The free flight allows pilots to choose their own routes, altitudes and speeds so that they have more freedom to optimize flight trajectories. But they are also responsible for the safe and fair resolution of trajectory conflicts. From this background, NASA is currently investigating a new concept of operations for the National Airspace System, designed to improve capacity while maintaining or improving current level of safety (Ref. 2). The concept, known as Distributed Air/Ground Traffic Management (DAG-TM), allows appropriately equipped autonomous aircraft to maneuver freely for flight optimization while resolving conflicts with the other traffic and staying out of special use airspace and hazardous weather (Ref. 5). The free flight

† 2007년 05월 01일 접수 ~ 2007년 09월 19일 심사완료
* 한국항공우주연구원, soojung@kari.re.kr
** 한국항공우주연구원, mklee@kari.re.kr
*** 한국항공우주연구원, oshtiger@kari.re.kr

concept seems to have many advantages, but its realization depends on the degree of safety guarantee which can be obtained from the enabling technologies such as Global Positioning System (GPS), data-link communication, Traffic Alert and Collision Avoidance System (TCAS), powerful on-board computational capability, and aircraft maneuverability.

Although many researches of the automated airspace were originally raised to resolve the manned air traffic congestion, recently the great strides of unmanned aerial vehicle (UAV) are pushing to solve the airspace conflict issue. The "see-and-avoid" is a primary restriction to normal operations of UAVs. The intent of the see-and-avoid is for pilots to use their sensors and other tools to find and maintain situational awareness of other traffics and to yield the right-of-way, in accordance with the rules, when there is a traffic conflict (Ref. 6). Also, FAA cites the requirement that UAV should detect, recognize, decide, and maneuver with at least the same capability as manned aircraft, and perform at least as well as if a pilot is onboard the UAV (Ref. 7). Eventually, the fully automated airspace concept free from collision accidents should be established before UAVs are to be utilized commercially and in public.

Recently, the tilt rotor has risen as a strong alternative for the future high speed VTOL aircraft in commercial as well as military applications. The tilt rotor UAV is ready to be put into practical application. However, the airspace issue is still a primary obstacle for the full commercial application of UAV. In this paper, among the collision avoidance procedures of UAV such as detection, recognition, decision, and maneuver, the maneuver capability of the tilt rotor UAV was investigated by numerical simulation methods.

II. Simulation Models and Methods

2.1 Tilt Rotor UAV

Figure 1 shows Smart Unmanned Aerial Vehicle (SUAV) that Korea Aerospace Research Institute (KARI) has developed for a robust and intelligent tilt rotor UAV exhibiting high-speed cruise and vertical take-off and landing capabilities since 2002. The nominal mission weight is 1,000kg. The length of air vehicle is 5m, and the maximum power of the engine is 560 hp. The maximum and maneuvering speeds are 475 km/h and 400 km/hr, respectively. Highly reliable design and operating concepts were implemented in the critical subsystems such as control and avionics systems. SUAV can fly in three flight modes, helicopter, conversion, and airplane modes like the other manned tilt rotor aircrafts. The typical mission of SUAV would be performed in airplane mode, since the primary mission of SUAV is reconnaissance and surveillance. The power plant located at center fuselage and driving both rotor systems through center and pylon gearboxes is P&W 206C turbo shaft engine. Static and dynamic wind tunnel tests with and without proprotor have been performed to gather aerodynamic performance and stability & control data. Figure 2 shows a wind tunnel test model of SUAV without proprotor installed in the test section of KARI subsonic wind tunnel.

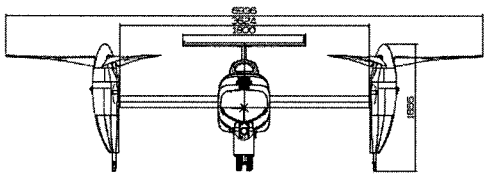

Figure 1. Front View of Smart UAV

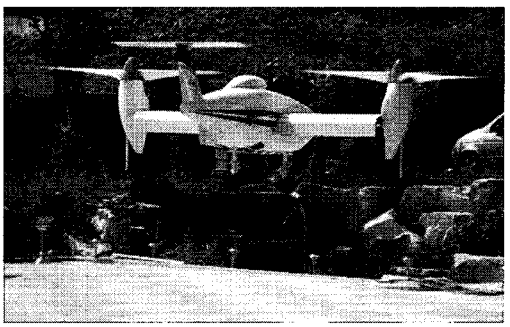

Figure 2. Smart UAV Flight Demonstrator

2.2 Numerical Methods

A six degree of freedom Tilt Rotor Flight Simulation code (TRFS code) was developed using time-accurate numerical integration scheme (Ref. 8). The time lagging scheme was applied to the second order coupled terms in the

governing equations of Eq. (1) in order to save the computational time. The time step applied to the simulation is 0.001 second. From the preliminary trade study, it was found that the time step higher than 0.001 second would give a unrealistic diverged solution, especially in the severe maneuver cases.

Nonlinear aerodynamic data generated from wind tunnel tests and computational fluid dynamics predictions were utilized in the simulation of Eq. (1). The propulsion performance data from P&W 206C engine deck was applied with nominal values of center of gravity and moment of inertia in airplane mode. Figure 3 shows the basic algorithm of TRFS code. The flight control parameters of SUAV are elevator, flaperon, engine throttle, and proprotor pitch. The flight simulation was restricted by the user-specified constraints of angle of attack, bank angle, engine power and torque, structural load factor, proprotor load, and actuator control performance.

$$
\begin{aligned}
&m(\dot{u} - vr + wr) = F_x \\
&m(\dot{v} + ur + wp) = F_y \\
&m(\dot{w} - uq + vp) = F_z \\
&I_{xx}\dot{p} - I_{xz}\dot{r} - I_{xz}pq + (I_{zz} - I_{yy})rq = L \\
&I_{yy}\dot{q} + (I_{xx} - I_{zz})pr + I_{xy}(p^2 - r^2) = M \\
&I_{zz}\dot{r} - I_{xz}\dot{p} + I_{xz}qr + (I_{yy} - I_{xx})pq = N
\end{aligned}
\tag{1}
$$

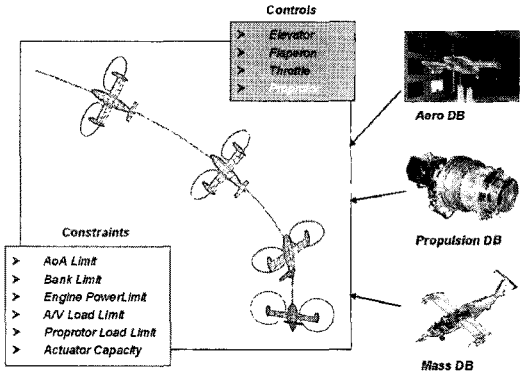

Figure 3. Numerical Simulation Algorithm

2.3 Collision Zone

There can be many kinds of collision objects for unmanned aerial vehicle. The first type of the collision object is non-moving one such as buildings, grounds including mountains and runways, storms, and something like that. Whereas, the second type is moving one such as manned aircrafts, UAVs, birds, et al. From the examples, the collision objects have various characteristics of speed and shape. To effectively investigate the collision avoidance capability of UAV in this paper, it was needed to simplify the various collision objects by a simple shape. It was also preferred the shape can be well applied in the manned airspace model.

Figure 4 shows the collision zone simulating the representative collision object to be avoided in this paper. It was defined that a collision, a near miss named in Ref. 2, occurs when the simulated flight path penetrates the collision zone of cylindrical geometry as shown in Figure 4. The baseline radius and height of the collision zone was referred from the manned airspace model in Ref. 2. The collision avoidance time (CAT) was defined by the minimum time needed to avoid contacting the collision zone with the maximum maneuver capability. That is, it is the minimum time without penetrating the collision zone from the time of collision avoidance maneuver activation. It means only the time consumed during the maneuver flight excluding the other collision avoidance behaviors such as detection, recognition, and decision.

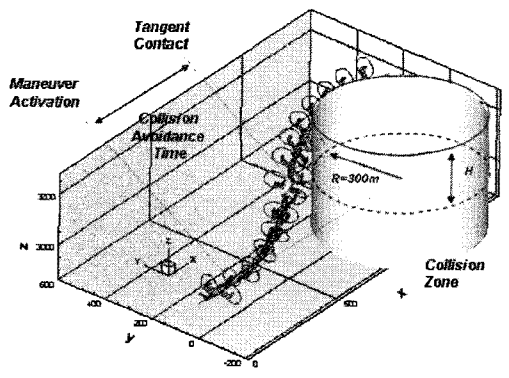

Figure 4. Collision Avoidance Definition

2.4 Collision Avoidance Maneuver

Figure 5 shows a standard priority of collision avoidance procedure generally applied

in the manned airspace (Ref. 7). The procedure is composed of the Scheduled Flight by Prescribed Rules, Air Traffic Control (ATC), TCAS, finally Detect, See and Avoid (DSA). SUAV can follow the general collision avoidance procedure in the manned airspace, because SUAV is being developed to incorporate the required options of collision avoidance system (CAS) as shown in Table 1. However, even if SUAV would equip the best collision avoidance system of cooperative type, it cannot be perfect because all the collision objects can not be incorporated by the required communication equipments for collision avoidance. As a result, DSA capability shall be an essential function to dominate the level of air traffic safety in the future.

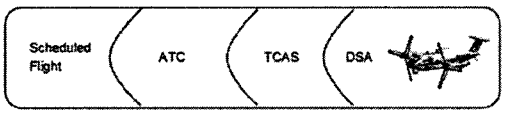

Figure 5. Priority of Collision Avoidance

Among the DSA category, investigating the "detect and see" capability is out of scope in this paper. Therefore, the "avoid" capability shall be investigated and discussed in this paper. The collision avoidance maneuver can be generally classified by two types of "pass" or "return" (Ref. 8). The return maneuver is needed when the obstacle stands in the whole foreground such as storm, gunfire, and terrain approach. The pass maneuver, more general case, can be classified by over-pass, side-pass, under-pass, and mixed-pass. In this paper, the collision avoidance maneuver of SUAV was confined to the pass maneuver. But, the terrain collision avoidance performance, which regarded as important in the approach condition of fixed wing aircraft, can be indirectly estimated from the over-pass (pull-up) maneuver simulation results.

Table 1. Collision Avoidance System Options

Type	Equipments
Non-Cooperative	EO/IR Camera, Radar
Cooperative	TCASII, ADS-B, Transponder

III. Simulation Conditions

3.1 Analysis Conditions

The baseline initial flight condition in the simulation was set on the steady level trimmed flight in airplane mode with 400 km/h speed at 3km altitude. For the flight control parameters, the commands of elevator, flaperon and engine throttle were selected as inputs, while the proprotor pitch was output. The initial engine throttle was set to keep the cruise level flight with the given speed and altitude. After the maneuver activation, the throttle increased to the maximum available value in two seconds, and then kept the maximum value during the maneuver. The collision avoidance maneuver was restricted by the SUAV flight envelope limits and specifications of control components as shown in Table 2. The realistic flight control commands from the actual actuator performance data were modeled and applied to the simulation. An artificial damping was not applied in order to avoid confusion in the analysis of simulation results.

Table 2. Flight Simulation Constraints

Flight Parameter	Limit
Angle of Attack	15 deg
Bank Angle	60 deg
Pitch Rate	20 deg/s
Roll Rate	50 deg/s
Structural Load Factor	2.8 g
Control Surfaces Speed	30 deg/s

3.2 Representative Maneuvers

Figure 6 shows four representative maneuver flights of SUAV for collision avoidance. The radius and height of collision zone are 300m and 100m, respectively. The control command inputs for the maneuvers are summarized in Table 3. For example, the maximum pull-up means the maneuver flight which can show the minimum collision avoidance time by the maximum available elevator control without exceeding the flight constraints as shown Table

2. The level turn maneuver in Table 3 means the turn flight with appropriate elevator control to keep the initial altitude.

It can be seen from Figure 6 that the maximum pull-up and the maximum pull-up turn maneuvers pass the upper boundary of the collision zone. Whereas, the moderate pull-up turn, the level and dive turn maneuvers pass the side surface of the collision zone. At this collision zone shape, the maximum pull-up maneuver using only elevator pitch control shows the minimum collision avoidance time as shown in Table 3. It is due to the shorter height of the collision zone relative to the radius. Here, the collision avoidance times were computed by approaching the collision zone from far backward to forward directions until it touches the flight path first. Figure 7 shows the computed air vehicle attitudes in the maneuver flights with the time interval of 0.5 second.

Table 3. Maneuver Control Definitions

Maneuver Type	Elevator	Aileron	CAT*
Max Pull-up	Max	No	4.2 s
Max Pull-up Turn	Max	Max	5.2 s
Moderate Pull-up Turn	Mod	Max	6.7 s
Level Turn	Little	Max	7.9 s
Dive Turn	No	Max	9.1 s

where,

Max : Magnitude of Maximum Available
Mod : Half Magnitude of Maximum Available
Little : Magnitude for Level Flight

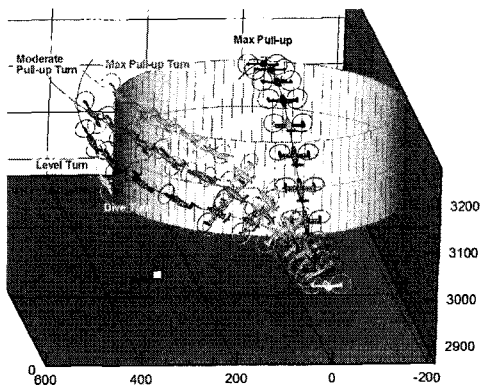

Figure 6. Representative Collision Avoidance Maneuvers (dt=1.0 s, R=300m, H=100m)

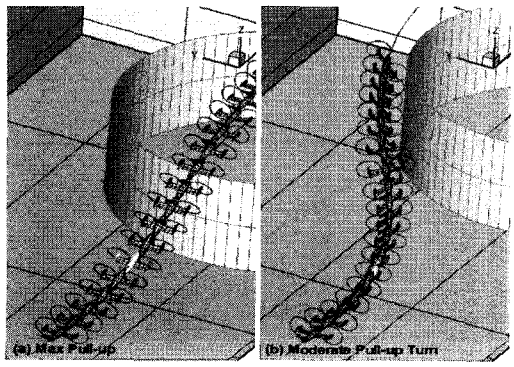

Figure 7. Air Vehicle Attitudes in Maneuvers (dt=0.5 s, R=300m, H=100m, Vi=400km/h)

IV. Simulation Results

4.1 Maneuver Characteristics

To verify the results of TRFS code, the same maneuver flights were simulated by CAMRADII code (Ref 9). Figure 8 shows the comparisons of both results for the maximum pull-up maneuver, and it shows good agreements. It

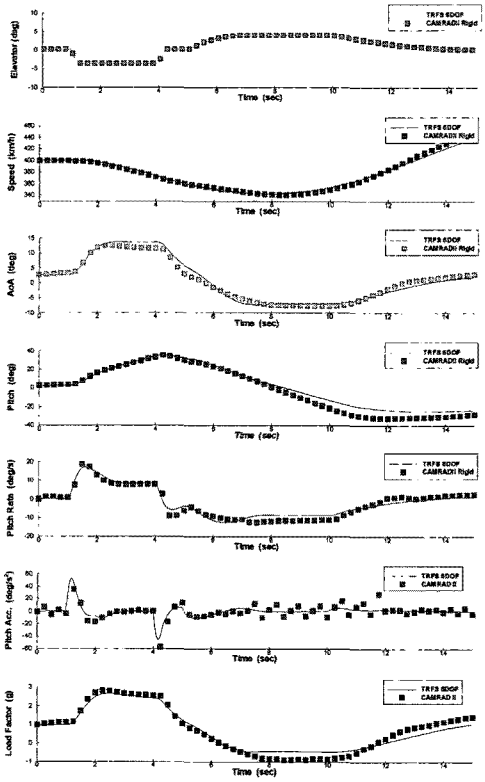

Figure 8. Comparison of Simulation Results by TRFS and CAMRAD II (Maximum Pull-up Maneuver, Vi=400km/h)

can be found that the angle of attack and structural load factor of both results kept under the permissible limits. Some overshoots in the pitch rate and acceleration can be found in Figure 8. They seem to be caused by lack of artificial pitch damping in the simulation, but it can be easily removed in both simulation and the real flight test if needed. A scattering tendency in the pitch acceleration of CAMRADII result seems to be due to relatively coarse time step of 0.01 second when compared with 0.001 second of TRFS, because it was needed much more computing time and power in CAMRADII analysis. The both TRFS and CAMRADII results in Figure 8 were from the rigid model assumption of proprotor blade.

SUAV has three blades of gimbaled hub system. Therefore, it should be checked whether the elastic effect of proprotor gives a significant influence on the maneuverability in spite of airplane mode. Figure 9 shows the computed results of rigid and elastic proprotor models by CAMRADII with the same control commands of TRFS. It shows acceptable agreements except small discrepancy around the maximum control command input region. It can be noted that the elastic model shows a little more conservative result than rigid model, because of the damping effect of elastic proprotor during the maneuver. It is also found that the pitch and load factor in the elastic case are lower than those of rigid cases as shown in Figure 9. As a result, the elastic effect gives a little longer collision avoidance time than the other two rigid methods as shown in Table 4.

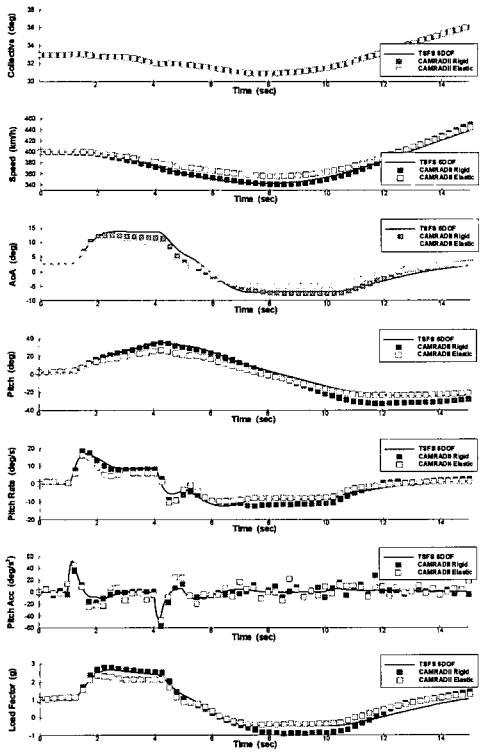

Figure 9. Comparison of Rigid and Elastic Proprotor Models (Maximum Pull-up Maneuver, Vi=400km/h)

Table 4. Estimated Collision Avoidance Time (MaxPull-up Maneuver, Vi=400km/h)

Method	CAT
TRFS Rigid	4.2 s
CAMRADII Rigid	4.1 s
CAMRADII Elastic	4.8 s

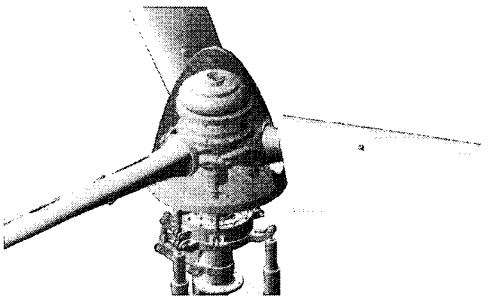

Figure 10. SUAV Proprotor

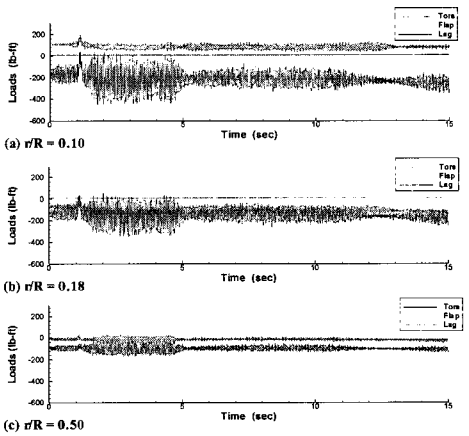

Figure11. Estimated Load Time Histories (Maximum Pull-up Maneuver, Vi=400km/h)

Figure 10 shows the SUAV proprotor system having three bladed, gimbaled, stiff-inplane rotor system. Figure 11 shows the computed loads time histories on three different spanwise locations of proprotor blade by CAMRADII with elastic proprotor model for the maximum pull-up maneuver flight. The spanwise locations of proprotor blade r/R=0.10 and r/R=0.18 in Figure 11(a) and Figure 11(b) are on the spindle flexure. As expected, the lag moment shows the highest values in both mean and oscillatory loads when compared with flap or torsion moments. It is noted from Figure 11 that the time histories of oscillatory lag moment show similar pattern with those of angle of attack and structural limit load factor distributions in Figure 9. It means that the proprotor oscillatory load is closely related to the maneuver flight characteristics. It was confirmed that the maneuver load analysis based on the standard mission spectrum satisfied the fatigue life requirement of SUAV proprotor system.

Although the elastic proprotor model can give more realistic solution including proprotor loads, it consumes huge computational time to give the same level of time accurate flight trajectory solution. Therefore, with the reasonable agreements as shown in Figure 9 and Table 4, most of collision avoidance maneuver simulations were performed by TRSF code with the rigid proprotor model.

4.2 Collision Avoidance Performance

Figure 12 shows the computed collision avoidance time for the five representative maneuvers as defined in Table 3. The initial cruise speed is 400km/h, and the collision zone has 300m/100m of radius/height cylindrical geometry. The collision zone is considered by a fixed, non-moving obstacle. The trend curve in Figure 12 shows that the collision avoidance time continuously increases as the pitch control reduces. The estimated collision avoidance times of the level turn and dive turn maneuvers show approximately twice magnitude of the maximum pull-up maneuver case. It may be natural because the radius of the collision zone is three times of the height in spite of considering the relatively low pitch control power capability than the roll control in SUAV. The relatively low pitch control power of SUAV is caused from the low stall limit due to the short wing span and low aspect ratio, when compared with the other fixed wing aircrafts. However, the bank and roll control limits of SUAV are relatively superior to the manned tilt rotor aircrafts. SUAV has two primary cruise speeds of 250km/h and 400km/h in Long endurance patrol (LEP) and Emergency Catch-Up (ECU) missions, respectively (Ref. 10). Although SUAV was designed to have the maneuvering speed of 400 km/h, it is important to investigate the maneuver performance at low cruise speed from the perspective of collision avoidance capability.

Figure 13 shows the collision avoidance time distributions according to various initial flight speeds. In all the computed maneuver cases, the collision avoidance times increase as the initial flight speeds decrease. For example, from the result of the maximum pull-up maneuver, the collision avoidance time from the initial speed 250 km/h shows about double of that from the

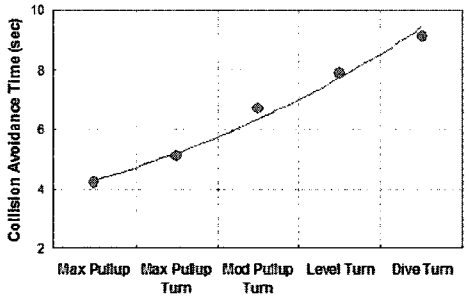

Figure 12. Computed CATs (Vi=400km/h)

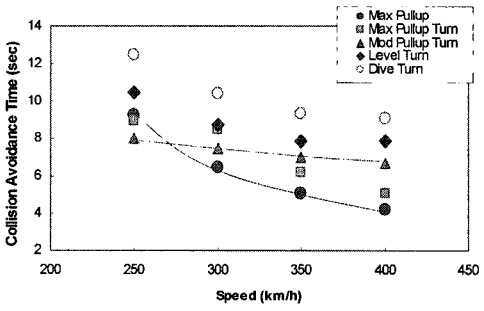

Figure 13. Effect of Initial Speed on CAT

initial speed 400km/h. This is not only due to the flight speed difference. Because, as mentioned earlier, the flight speed can be increased to the maximum available power by engine throttle control after the maneuver activation (1.0 second in reference time) as shown in Figure 14(c).

Figure 14(a) shows the time histories of flight speeds in the maximum pull-up maneuver starting from four different initial flight speeds. The low speed cruise (Vi=250km/h) case shows that the flight speed increases after the maneuver activation, in opposition to the high speed cruise case (Vi=400km/h). The main reason of such a high collision avoidance time in the low initial flight speed is the angle of attack limit. The low flight speed has relatively small angle of attack margin to the stall limit. For example, the low speed cruise case (Vi=250km/h) in Figure 14(b) shows little margin for pitch control, while the high speed cruise case (Vi=40km/h) has enough. As a result, the elevator pitch control is restricted to only a small deflection in the low speed maneuver. Here, the flap deflection can be one of solution to enhance the stall limit in the low speed maneuver. However, it has a disadvantage of decreasing the flight speed.

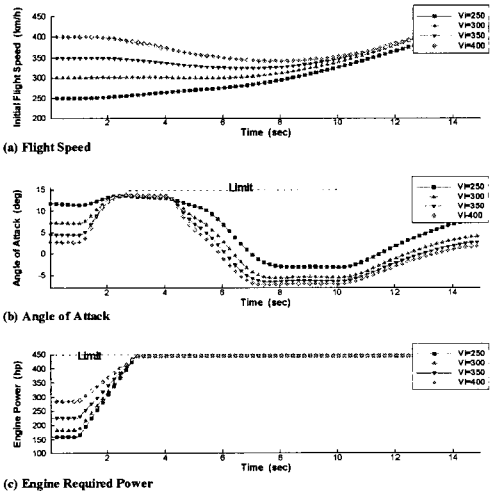

Figure 14. Computed Flight Parameters (Maximum Pull-up Maneuver)

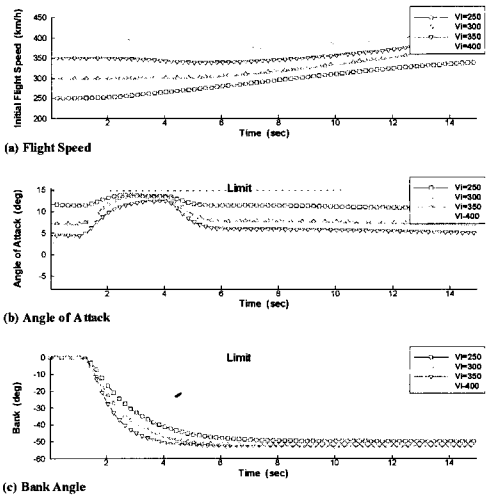

Figure 15. Computed Flight Parameters (Moderate Pull-up Turn Maneuver)

It can be noted from Figure 13 that the moderate pull-up turn maneuver shows a very low slope of trend curve to the initial flight speed. This means that the initial flight speed cannot be a primary factor to determine the collision avoidance time. Figure 15(b) shows slow increases of angle of attack after the maneuver activation in the moderate pull-up maneuver, while the maximum pull-up shows very steep increases as shown in Figure 14(b). Because the elevator deflection angle engaged in the moderate pull-up turn maneuver was half magnitude of that used in the maximum pull-up maneuver. It is noted from Figure 14(b) and Figure 15(b) that the angle of attack distributions in the moderate pull-up turn maneuver shows relatively much evener than those of the maximum pull-up maneuver.

The effect of the initial flight speed on the collision avoidance time is summarized in Figure 16. The trend curve in high speed is continuously increasing pattern as shown in Figure 16(a), while it shows a concave curve having the minimum location at the moderate pull-up turn maneuver in low speed. Figure 16(b) shows the sensitivity of the initial flight speed variation on the collision avoidance time from the high cruise speed (400km/h) to the low cruise speed (250 km/h). The maximum pull-up and the maximum pull-up turn

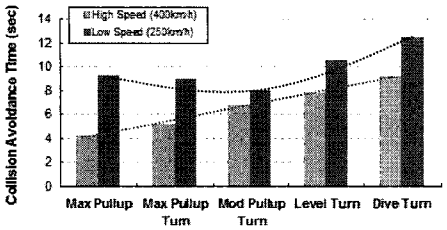

(a) CATs bt Initial Cruise Speeds

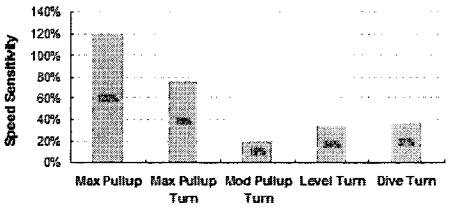

(b) Speed Sensitivity on CAT

Figure 16. Effect of Initial Cruise Speed on CAT

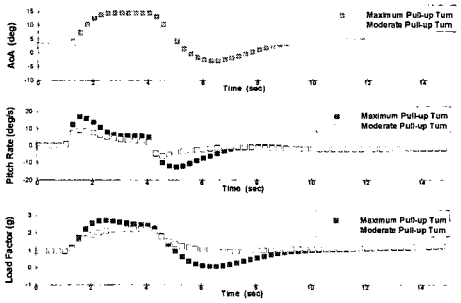

Figure 17. Comparison of Maximum and Moderate Pull-up Turn Maneuvers (Vi=400km/h)

maneuvers show very high level of sensitivity when compared with the other maneuvers. This means that the speed sensitivity of collision avoidance time mainly depends on the pitch maneuver. It is also noted from Figure 16(b) that the moderate pull-up turn maneuver shows the lowest magnitude of speed sensitivity.

For the pull-up turn maneuvers, Figure 13 shows that the maximum pull-up turn is better collision avoidance capability than the moderate pull-up maneuver in high speed, while is worse in low speed. The difference of the two maneuvers is the amount of elevator deflection for pitch control as defined in Table 3. Although the maximum pull-up turn maneuver shows superior collision avoidance capability than the moderate pull-up turn maneuver in high speed, the reduction of the pitch control magnitude in the moderate pull-up turn gives very softened flight characteristics as shown in Figure 17. The alleviation of the pitch rate and load factor as shown in Figure 17 can give a significant advantage in the structural design of proprotor and air vehicle.

4.3 Effect of Collision Shape

Figure 18 shows the computed collision avoidance time for three different shapes of collision zone as defined in Figure 4. The radius was fixed by 100m, and the heights were 100m, 200m, 300m, respectively. The aspect ratio, defined as the ratio of height to radius, of three cases are 0.33, 0.67, and 1.0. Although it doesn't generally need to consider the collision zone of high aspect ratio in the mid air-to-air collision, it is meaningful to investigate the effect on the collision avoidance time in the other collision cases. As shown in Figure 18(a), the result of 100m height collision zone shows continuously increasing pattern of collision avoidance time. However, the trend curve changes from linear shape to concave curve as the aspect ratio of the collision zone goes to 0.67 and 1.0. From Figure 18(a), the boundary aspect ratio the trend curve shape changes is approximately 0.5. In other words, the linear shape changes to the concave shape when the aspect ration goes over 0.5. The concave curve has the lowest point at the moderate pull-up turn maneuver. This trend was seen from the low speed maneuver in Figure 16(a).

The latter three maneuvers in Figure 18, moderate or no pull-up, show constant collision avoidance times in spite of the collision zone shape change. Because the flight paths of the maneuvers pass the side face of collision zone. Whereas, the maximum pull-up and the maximum pull-up turn maneuvers show that the aspect ratio increase of collision zone gives a big impact on collision avoidance time, because the flight paths pass the upper boundary of collision zone. As a result, in the

maximum pull-up maneuver, the collision avoidance time continuously increases as the aspect ratio of collision zone increases. Figure 18(b) shows the sensitivity of collision zone aspect ratio on collision avoidance time. The maximum pull-up shows the highest value of sensitivity, while the latter three maneuvers show no sensitivity. From theses results, it can be said that the moderate pull-up turn maneuver is the most robust and efficient maneuver for collision avoidance from the perspective of variable collision object shape. This statement sounds more reasonable especially in UAV applications. Because, in many UAV applications, there are common affairs that the obstacle shape cannot be exactly grasped and therefore right decision making is not available in a brief instant.

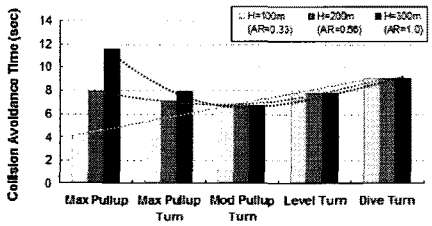

(a) CATs by Collision Zone Heights

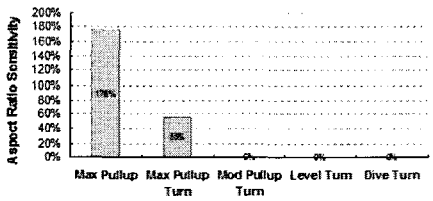

(b) Collision Zone Aspectio Ration Sensitivity

Figure 18. Effect of Collision Zone Shapeon CAT (Vi=400km/h, R=300m)

4.4 Collision Avoidance Maneuver for Moving Obstacles

The five collision avoidance scenarios for moving obstacles were defined as shown in Figure 19. The five cases of intruder airplane motions were modeled ; (a) opposite approach, (b) overtaking approach, (c) side approach, (d) descending approach, (e) climbing approach. It was found that the turn maneuver was the most efficient for the opposite and overtaking

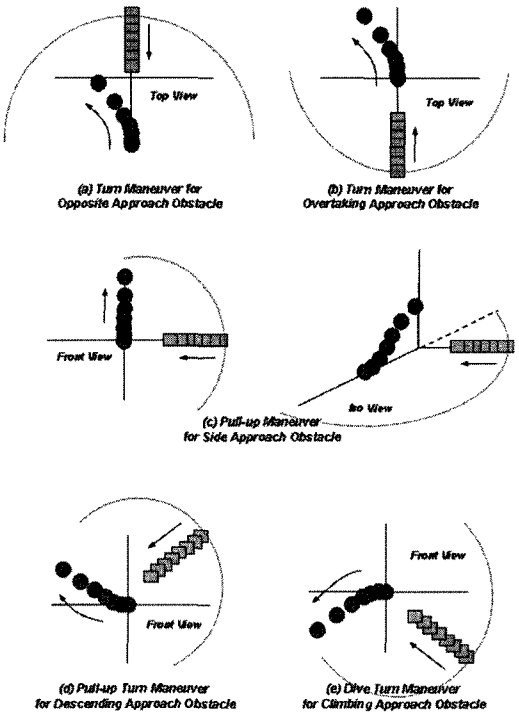

Figure 19. Collision Avoidance Scenario for Moving Obstacles

approach cases as shown Figure 19(a) and 19(b). The pull-up maneuver was the best for the side approach intruder, while the pull-up and dive turn maneuvers were for the descending and the climbing approach intruders, respectively.

Figure 20(a) shows the simulated trace of moderate pull-up turn maneuver to avoid the intruder approaching from the opposite direction. The flight simulation conditions and collision zone definition were the same with the stationary cases. The intruder was assumed to approach with constant level flight from the opposite direction. The flight speeds of host and intruder airplanes were set by several values of wide range as shown in Figure 20(b). The required collision detection distance in the vertical axis of Figure 20(b) was defined by the minimum distance to avoid the collision with the intruder. The higher value of the required collision detection distance means the lower performance of collision avoidance. Figure 20(b) shows the required collision detection distance distributions for the various speed values of host and intruder airplane. From the simulated

results in Figure 20(b), it can be said that the required collision detection distance was little affected in most of the host speed conditions. On the other hand, the intruder speed gave a direct influence on the required collision detection distance.

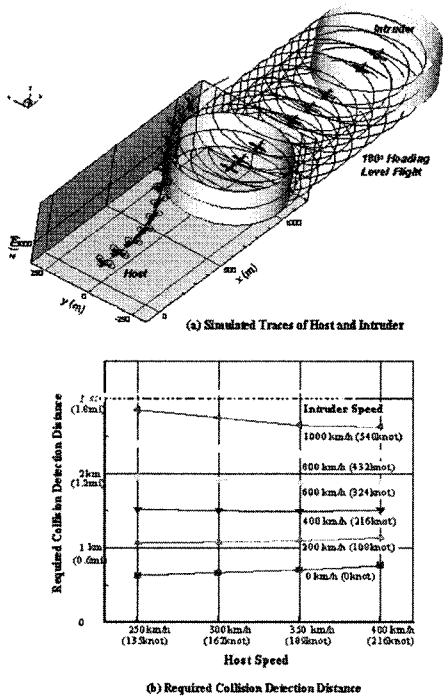

Figure 20. Collision Avoidance Simulation for Opposite Approach Intruder

Figure 21 shows the simulation results for the moving obstacle from the side direction. The maximum pull-up maneuver showed the best collision avoidance performance in this case. Figure 21(b) shows that the host speed gave a big influence on the required collision detection distance. Especially, the influence is big in the low host speed. This reason can be explained as described with Figure 16. It is because the pull-up maneuver shows the highest sensitivity of host speed on the collision avoidance performance. And, it could be noted that this tendency was more clearly seen as the intruder speed went higher. The collision avoidance performance was rapidly improved as the host speed went higher under the high intruder speed condition.

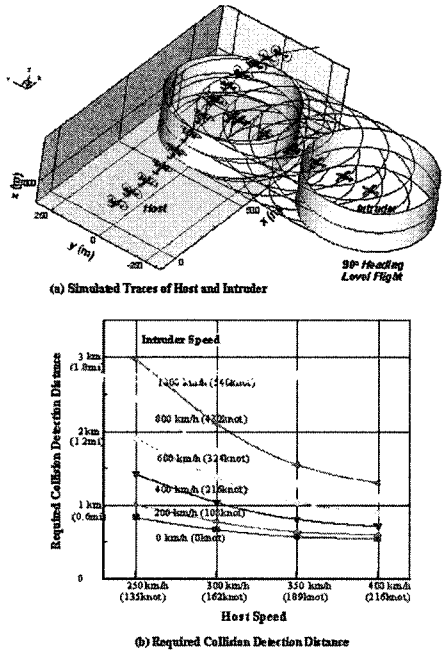

Figure 21. Collision Avoidance Simulation for Side Approach Intruder

Figure 22 shows the maximum pull-up turn simulation for the intruder descending from 135 degree opposite direction. The descent angle of

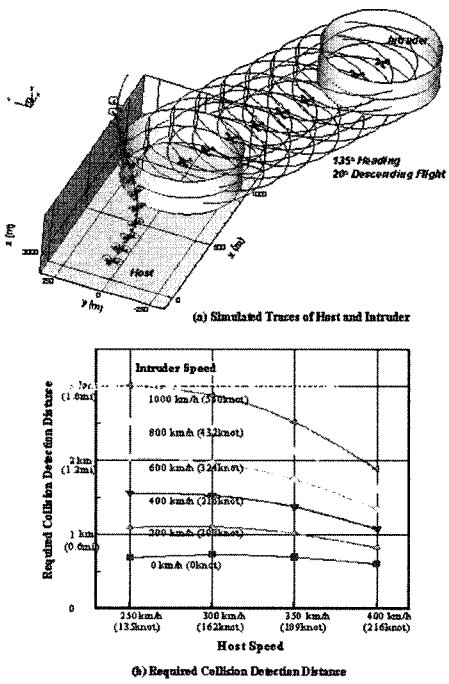

Figure 22. Collision Avoidance Simulation for Descending Approach Intruder

the

intruder was 20 degree. In this case, the maximum pull-up turn maneuver was the most efficient for the collision avoidance. Figure 22(b) shows similar trend that the collision avoidance performance was improved as the host speed went higher. But, it was interesting that the characteristic curves of the required collision detection distance show convex type whereas those in the case of side approach intruder were concave. Figure 23 shows the simulation results for the climbing approach intruder. The intruder was assumed by climbing with 20 degree of climb path and 45 degree of heading angle. The dive turn maneuvers were selected and simulated to avoid the approaching intruder. The computed characteristic curves of the required collision detection distance show similar trend with the case of side approach intruder, but the slope of curves were smoother. It could be noted that the characteristic curves have the minimum inflection points at the specific combinations of host and intruder speeds.

From these simulation results for moving obstacles, it can be found that the required collision detection distances of SUAV are within 3km if not considering the supersonic intruder. It can be under 2km if the intruder speed is lower than 500km. And, the required collision detection distance are generally decreased as the host speed goes higher. That is, the speed up of host speed can improve the collision avoidance performance. The degree of the improvement can be different by the collision avoidance cases. It should be noted that the required collision detection distance mentioned in this paper included only the estimated values of airplane maneuver performance except detection, recognition and decision.

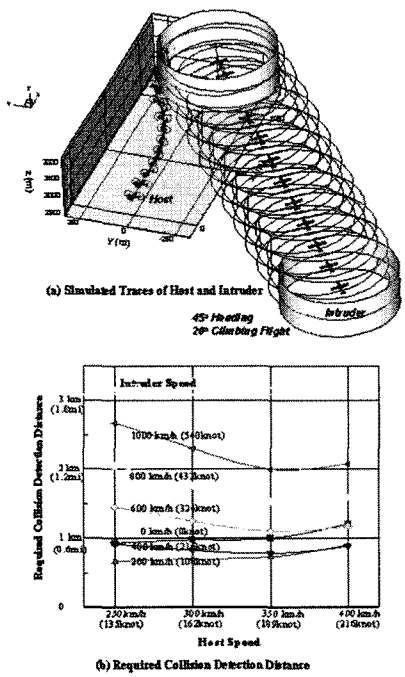

(a) Simulated Traces of Host and Intruder

(b) Required Collision Detection Distance

Figure 23. Collision Avoidance Simulation for Climbing Approach Intruder

V. Conclusion

The collision avoidance maneuver flights of unmanned tilt rotor aerial vehicle were simulated by numerical integration method. From the analysis results, following conclusions can be obtained.

1) The pitch control is the most primary factor to determine the collision avoidance time at the high speed cruise condition under the assumption of cylindrical shaped collision zone.

2) The maximum pull-up maneuver shows the highest sensitivity of flight speed on collision avoidance time, while the moderate pull-up turn maneuver shows the lowest. The angle of attack margin to stall limit is the most important factor to determine the collision avoidance time in low speed flight condition.

3) The maximum pull-up maneuver shows the highest sensitivity of collision zone shape on collision avoidance time. The trend curve of collision avoidance time changes from linear to concave when the aspect ratio of collision zone goes over 0.5.

4) It can be said that the moderate pull-up turn maneuver is the most robust and efficient collision avoidance maneuver at the various flight speeds and collision object shapes in tilt

rotor UAV applications.

5) It was found that there needed at least 3 km for the required collision detection distance in the most cases of moving intruder speed and route.

Reference

[1] Heinz Erzberger, "The Automated Airspace Concept", 4th USA/Europe Air Traffic Management R&D Seminar, Santa Fe, December 2001.

[2] Richard Barhydt, et al., "Regaining Lost Separation in a Piloted Simulation of Autonomous Aircraft Operations," 5th UAS/Europe ATM R&C Seminar, Budapest, Hungary, 2003

[3] Mieke Massink and Nicoletta De Francesco, "Modeling Free Flight with collision Avoidance," 7th IEEE International Conference on Engineering of Complex Computer Systems, 2001

[4] Radio Technical Commision for Aeronautics, "Final Report on RTCA Task Force 3 : Free Flight Implementation," Technical Report, RTCA, Washington DC., 1995

[5] NASA, "Concept Definition for Distributed Air/Ground Traffic Management (DAG-TM)," Version 1.0, 1999

[6] Office of the Secretary of Defense, "Airspace Integration Plan for Unmanned Aviation," Nov. 2004.

[7] James Utt, "Detect and Avoid (DAA) for Global Hawk and Predator," TAAC 2003 UAV Conference, October 2003

[8] Soojung Hwang, et al., "Evaluation of Collision Avoidance Maneuver for Smart UAV," 2005 KSAF Conference, Korea, 2005

[9] Wayne Johnson, "CAMRADII : Comprehensive Analytical Model of Rotorcraft Aerodynamics and Dynamics," Users Manual Release 4.3, Johnson Aeronautics, 2004.

[10] SUDC, "Standard Mission Profiles of Smart UAV," SUAV Program PDR Meeting, Daejeon, Korea, 2003